

The MACRO Experiment at Gran Sasso

G. Giacomelli and A. Margiotta

Dipartimento di Fisica dell'Università di Bologna and INFN, 40127 Bologna, Italy

Charles Peck - Fest, Caltech, 2005 *

Abstract

In this overview of the MACRO experiment we recall the structure of the detector and discuss several physics topics: atmospheric neutrinos and neutrino oscillations, high energy neutrino astronomy, searches for WIMPs and for low energy stellar gravitational collapse neutrinos, stringent upper limits on GUT magnetic monopoles, high energy downgoing muons, primary cosmic ray composition and shadowing of primary cosmic rays by the Moon and the Sun.

1 Introduction

MACRO was a large area multipurpose underground detector designed to search for rare events and rare phenomena in the penetrating cosmic radiation. It was optimized to look for the supermassive magnetic monopoles predicted by Grand Unified Theories (GUT) of the electroweak and strong interactions; it could also perform measurements in areas of astrophysics, nuclear, particle and cosmic ray physics. These include in particular the study of atmospheric neutrinos and neutrino oscillations, high energy neutrino astronomy, indirect searches for WIMPs, studies of various aspects of the high energy underground muon flux (which is an indirect tool to study the primary cosmic ray composition), searches for rare particles that may exist in the cosmic radiation.

The experiment was located in Hall B of the underground Gran Sasso Lab and started data taking with part of the apparatus in 1989; it was completed in early 1995 and was running in its final configuration until the end of 2000. The detector had global dimensions of $76.6 \times 12 \times 9.3 \text{ m}^3$ and provided a total acceptance of $\sim 10000 \text{ m}^2 \text{ sr}$ to an isotropic flux of particles. The detector had a modular structure: it was divided into six sections referred to as supermodules. The average rock overburden was $\simeq 3700 \text{ m.w.e.}$, while the minimum was 3150 m.w.e. This defines the minimum muon energy at the surface as $\sim 1.3 \text{ TeV}$ in order to reach MACRO.

It may be worth pointing out that all the physics and astrophysics items proposed in the 1984 Proposal were covered and good results were obtained on each of them, even beyond the most rosy anticipations [1]-[50].

The collaboration consisted of ~ 140 physicists and engineers from 6 Italian and 6 US Institutions, 1 Moroccan group and visitors from various developing countries. The complete list of names can be found in Ref. [10], [35], [50]. There was a close cooperation with the EASTOP Collaboration which operated an Extensive Air Shower Array at Campo Imperatore.

*The meeting was organized by Douglas Michael, who later passed away. Doug was one of the leaders of MACRO.

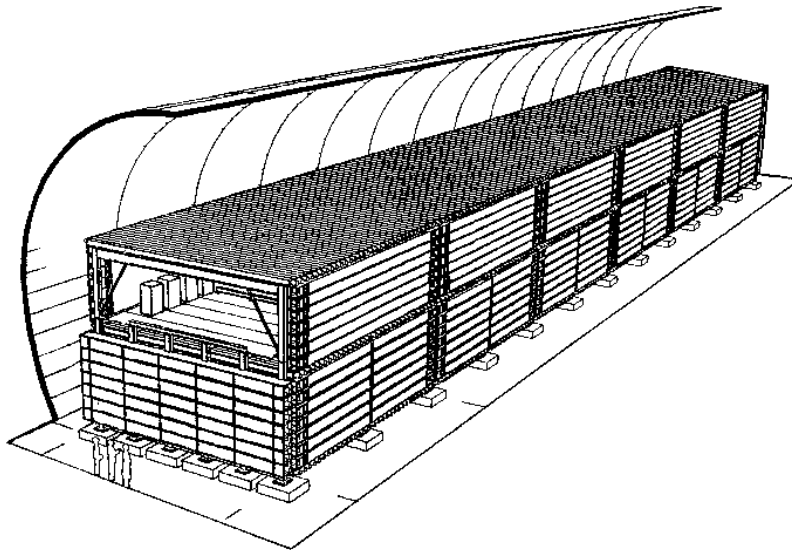


Figure 1: Layout of the MACRO detector which was installed in Hall B of the LNGS. Overall dimensions of the active part were $76.5 \times 12 \times 9.3 \text{ m}^3$ [35].

2 The Detector

Redundancy and complementarity were the primary goals in designing the experiment. Since few events were expected, multiple signatures and ability to perform cross checks with various parts of the apparatus were important. The detector was composed of three sub-detectors: liquid scintillation counters, limited streamer tubes and nuclear track detectors [16][35]. Each one of them could be used in “stand-alone” and in “combined” mode. The layout of the experiment is shown in Fig. 1. Notice the division in the *lower* and in the *upper* part (this was often referred to as the *Attico*); the inner part of the *Attico* was empty and lodged the electronics. Fig. 2 shows a cross section of the apparatus.

The scintillation subdetector. Each supermodule contained 77 scintillation counters, divided into three horizontal planes (bottom, center, and top) and two vertical planes (east and west). The lower part of the north and south faces of the detector were covered by vertical walls with 7 scintillators each; the upper parts of these faces were open to allow access to the readout electronics. The active volume of each horizontal scintillator was $11.2 \times 0.73 \times 0.19 \text{ m}^3$, while for the vertical ones it was $11.1 \times 0.22 \times 0.46 \text{ m}^3$. All scintillator boxes were filled with a mixture of high purity mineral oil (96.4 %) and pseudocumene (3.6 %), with an additional 1.44 g/l of PPO and 1.44 mg/l of bis-MSB wavelength shifters. The horizontal counters were seen by two 8" photomultipliers (PMTs) and the vertical counters by one 8" PMT at each end. The total number of scintillators was 476 with a total active mass of $\simeq 600$ tons. Minimum ionizing muons, when crossing vertically the 19 cm of scintillator, released an average energy of $\simeq 34 \text{ MeV}$ and were measured with a timing and longitudinal position resolution of $\simeq 500 \text{ ps}$ and $\simeq 10 \text{ cm}$, respectively.

The scintillation counters were equipped with specific triggers for rare particles, muons and low energy neutrinos from stellar gravitational collapses. The Slow Monopole Trigger (SMT) was sensitive to MMs with velocities from $10^{-4}c$ to $10^{-2}c$, the Fast Monopole

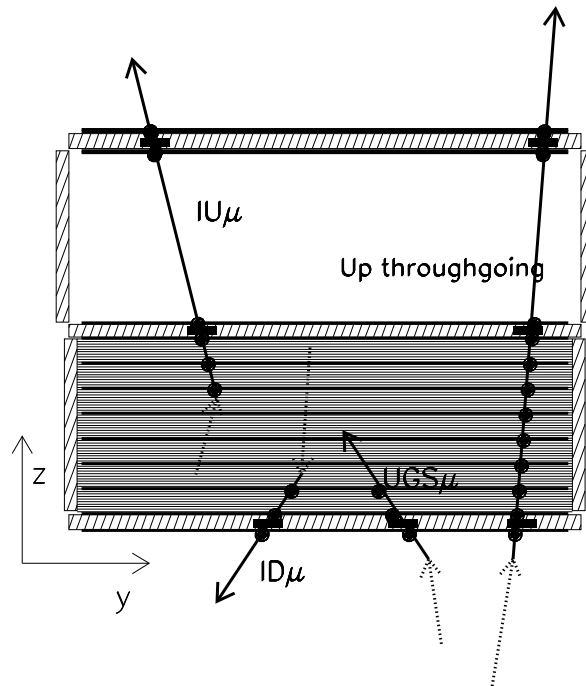


Figure 2: Vertical cross section of the detector and sketch of different event topologies induced by ν_μ interactions in or around MACRO. The black points and the black rectangles represent streamer tubes and scintillator hits, respectively. Tracking was performed by the streamer tubes; the time-of-flight of the muons was measured by the scintillators for *Up Semiconained* (Internal upgoing - IU μ) and *Up throughgoing* events (and also for downgoing muons).

Trigger (FMT) to poles with velocities from $5 \times 10^{-3}c$ to $5 \times 10^{-2}c$, the Lightly Ionizing Particle trigger was sensitive to fractionally charged particles, the Energy Reconstruction Processor (ERP) and “CSPAM” were primarily muon triggers (but used also for relativistic monopoles) and the gravitational collapse neutrino triggers (the Pulse Height Recorder and Synchronous Encoder –PHRASE– and the ERP) were optimized to trigger on bursts of low energy events in the liquid scintillators. The scintillator system was complemented by a 200 MHz waveform digitizing (WFD) system used in rare particle searches, and in any occasion where knowledge of the PMT waveform was useful.

The streamer tube subsystem. *The lower part* of the detector contained 10 horizontal planes of limited streamer tubes, the middle 8 of which were interleaved by 7 rock absorbers (total thickness $\simeq 360 \text{ g cm}^{-2}$). These set a $\simeq 1 \text{ GeV}$ energy threshold for muons vertically crossing the lower part of the detector. At the top of the *Attico* there were 4 horizontal streamer tube planes, 2 above and 2 below the top scintillator layer. On each lateral wall 6 streamer tube planes sandwiched the corresponding vertical scintillator plane (3 streamer planes on each side). Each tube had a $3 \times 3 \text{ cm}^2$ cross section and was 12 m long. The total number of tubes was 50304, all filled with a gas mixture of *He* (73 %) and n-pentane (27 %). They had $100\mu \text{ Cu/Be}$ wires and stereo pickup strips at an angle of 26.5° . The tracking resolution of the streamer tube system was $\simeq 1 \text{ cm}$, corresponding to an angular accuracy of $\simeq 0.2^\circ$ over the 9.3 m height of MACRO. The real angular resolution was limited to $\simeq 1^\circ$ by multiple Coulomb scattering of muons in the rock above the detector. The streamer tubes were read by 8-channel cards (1 channel for each wire) which discriminated the signals and sent the analog information (time development and total charge) to an ADC/TDC system (the QTP). The signals were used to form 2 different chains (Fast and Slow) of pulses, which were the inputs for the streamer tube Fast

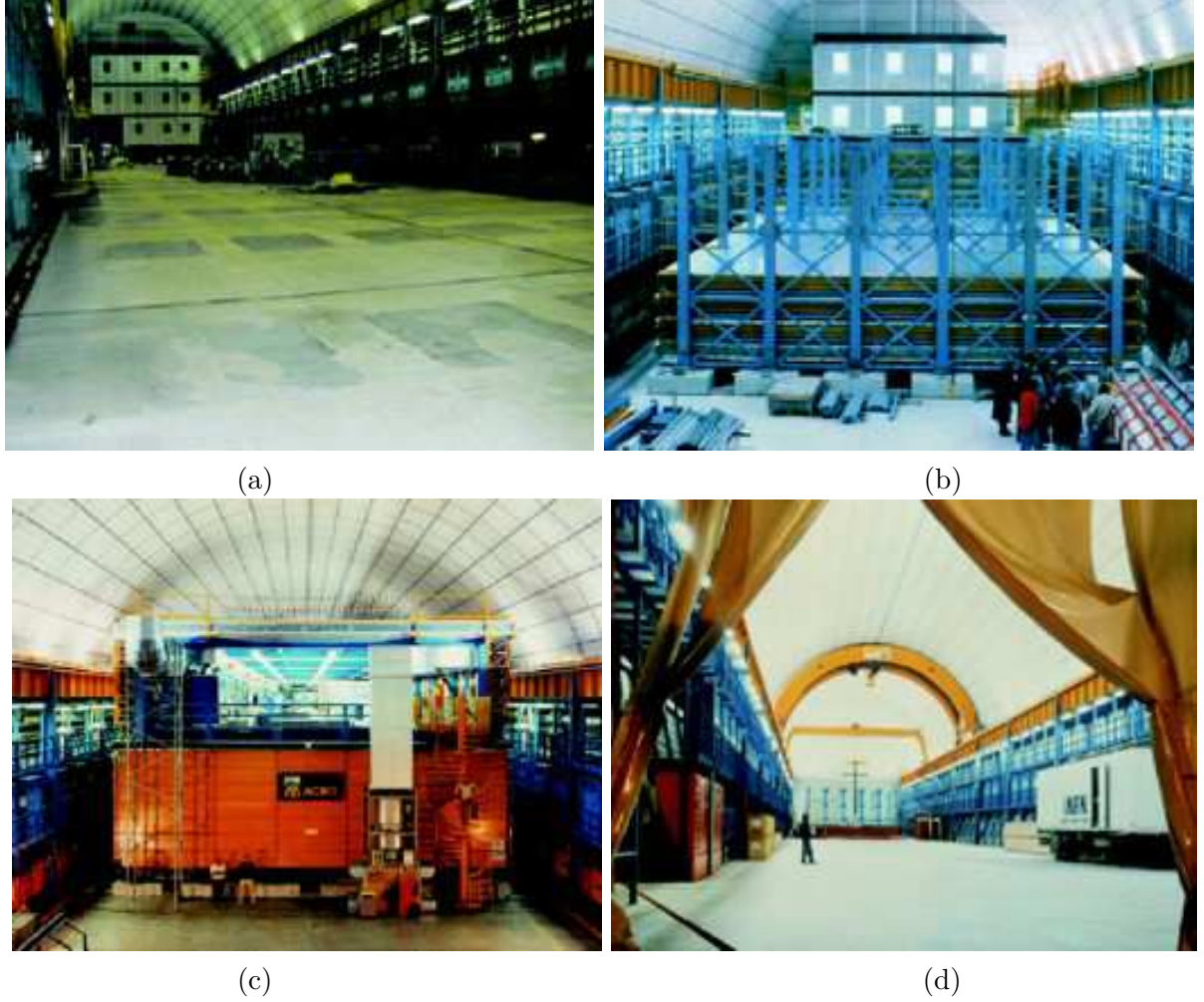


Figure 3: Hall B: (a) in 1987 just before starting construction; (b) in 1990 when the first lower supermodule was taking data while the second and third were under construction; (c) in 1995 when the completed MACRO detector started data taking (safety stairs and a ventilation system were added later); (d) Hall B empty in 2001.

and Slow Particle Triggers. In the 11 years of operation only 50 wires were lost.

The nuclear track subdetector was deployed in three planes, horizontally in the center of the lower section and vertically on the East and North faces. The detector was divided in 18126 modules, which could be individually extracted and substituted. Each module ($\sim 24.5 \times 24.5 \times 0.65 \text{ cm}^3$) was composed of three layers of CR39, three layers of Lexan and 1 mm Aluminium absorber to stop nuclear fragments.

The Transition Radiation Detector (TRD) was installed inside the *Attico*. It was composed of 3 modules (overall dimensions $6 \times 6 \times 2 \text{ m}^3$) and it was made of 10 cm thick polyethylene foam radiators and proportional counters filled with Ar (90 %) and CO_2 (10 %). The TRD measured muon energies in the range $100 \text{ GeV} < E_\mu < 930 \text{ GeV}$; muons of higher energies were counted.

Fig. 3 shows four photographs of Hall B taken from its south side. Fig. 4 shows a “group” of 11 downgoing muons.

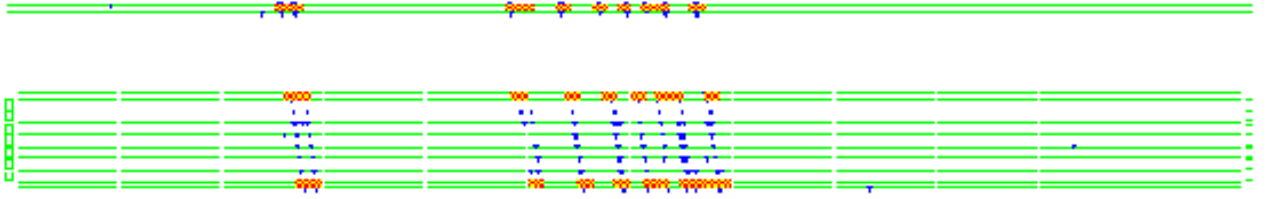


Figure 4: MACRO Event Display: lateral view of a group of 11 downgoing muons.

3 Atmospheric neutrino oscillations

A high energy primary cosmic ray (CR), proton or nucleus, interacts in the upper atmosphere producing a large number of charged pions and kaons, which decay yielding muons and muon neutrinos; also the muons decay yielding ν_μ and ν_e . The ratio of the numbers of ν_μ to ν_e is $\simeq 2$ and $N_\nu/N_{\bar{\nu}} \simeq 1$. Atmospheric neutrinos are produced in a spherical surface at 10-20 km above ground and they proceed towards the earth.

If neutrinos have non-zero masses, one has to consider the *weak flavour eigenstates* ν_e , ν_μ , ν_τ and the *mass eigenstates* ν_1 , ν_2 , ν_3 . The flavour eigenstates are linear combinations of the mass eigenstates. For 2 flavour (ν_μ , ν_τ) and 2 mass eigenstates (ν_2 , ν_3)

$$\begin{cases} \nu_\mu = \nu_2 \cos \theta_{23} + \nu_3 \sin \theta_{23} \\ \nu_\tau = -\nu_2 \sin \theta_{23} + \nu_3 \cos \theta_{23} \end{cases} \quad (1)$$

where θ_{23} is the mixing angle. The survival probability of the ν_μ "beam" is

$$P(\nu_\mu \rightarrow \nu_\mu) = 1 - \sin^2 2\theta_{23} \sin^2 \left(\frac{1.27 \Delta m^2 \cdot L}{E_\nu} \right) \quad (2)$$

where $\Delta m^2 = m_3^2 - m_2^2$, L is the distance travelled by the ν from production to detection.

Atmospheric neutrinos are well suited for the study of neutrino oscillations, since they have energies E_ν from a fraction of GeV up to more than 100 GeV and they travel distances L from few tens of km up to 13000 km; thus L/E_ν ranges from ~ 1 km/GeV to $\sim 10^5$ km/GeV. They are particularly useful to study oscillations for small Δm^2 , while matter effects can be studied with their high energy components.

The early water Cherenkov detectors and the tracking calorimeters measured ν_μ and ν_e charged current (CC) interactions. The results were expressed in terms of the double ratio $R' = R_{obs}/R_{MC}$, where $R_{obs} = (N_{\nu_\mu}/N_{\nu_e})_{obs}$ is the ratio of observed μ and e events and $R_{MC} = (N_{\nu_\mu}/N_{\nu_e})_{MC}$ is the same ratio for Monte Carlo (MC) events. The R' ratios from IMB [51] and Kamiokande [52] were smaller than expectations, while NUSEX [53], Frejus [54] and Baksan [55] did not find any deviation. Later, the Soudan 2 tracking and shower calorimeter detector confirmed the anomaly in the ν_μ/ν_e double ratio for contained events [56]. MACRO reported in 1995 a measurement of upthroughgoing muons from ν_μ of $\langle E_\nu \rangle \sim 50$ GeV, in which there was an anomalous zenith distribution and a deficit in the total number of observed upgoing muons [17]. In 1998 Soudan 2, MACRO and SuperKamiokande (SK) provided strong indications in favour of $\nu_\mu \longleftrightarrow \nu_\tau$ oscillations [57][25][58][59]. Later new results were presented by the 3 experiments and by others [60].

MACRO detected upgoing ν_μ 's via CC interactions $\nu_\mu \rightarrow \mu$; upgoing muons were identified with the streamer tube system (for tracking) and the scintillator system (for time-of-flight measurement). The events were classified in different categories:

Upthroughgoing muons ($E_\mu > 1$ GeV) come from interactions in the rock below the detector of ν_μ with $\langle E_\nu \rangle \sim 50$ GeV. The MC uncertainties arising from the neutrino flux, cross section and muon propagation on the expected flux of upthroughgoing muons were estimated to be $\sim 17\%$; this systematic error is mainly a scale uncertainty.

In order to verify that different flux simulations affect the zenith distribution at the level of only a few percent (while there is an effect of the order of $\sim 25\%$ on the event rates) MACRO compared data with the predictions of the Bartol96 [61], FLUKA [64] and HKKM01 [63] MCs, see fig. 5a. The shape of the angular distribution and the absolute value strongly favour neutrino oscillations with $\Delta m^2 = 0.0023$ eV² and maximum mixing. The absolute values of the MACRO upthroughgoing muon data are 25% higher than those predicted by the FLUKA and HKKM01 MC, while the shapes of the oscillated and non oscillated angular distributions from the different MCs agree within 5%.

A similar situation is found in the SK data [58]. The electron-like events were in agreement with the HKKM95 [62] MC predictions in absence of oscillations, while they are higher than the HKKM01 [63] non oscillated MC. For muon-like events, the new MC predictions are low for the SK data, especially for upthroughgoing muons. Previous comparisons between the SK muon data and the HKKM95 predictions had shown a global deficit of events and a zenith distribution shape in agreement with $\nu_\mu \longleftrightarrow \nu_\tau$ oscillations [58].

The difference between the new and old MC predictions is probably due to the use of a new fit of the cosmic ray data [65]. Recent results by the L3C and BESS experiments [66] on the primary cosmic ray fit show good agreement with the Bartol96 and HKKM95 predictions and a disagreement with the new fit of the cosmic ray data [65].

Low energy events. *Semicontained upgoing muons* (IU) come from ν_μ interactions inside the lower apparatus. *Up stopping muons* (UGS) are due to external ν_μ interactions yielding upgoing muons stopping in the detector; the *semicontained downgoing muons* (ID) are due to downgoing ν_μ 's with interaction vertices in the lower detector; the lack of time information prevents to distinguish between the two subsamples. An almost equal number of UGS and ID events is expected. The average parent neutrino energy for all these events is 2-3 GeV. The angular distributions are compared with MC predictions without oscillations in Figs. 5b,c. Our low energy data show a uniform deficit over the whole angular distribution with respect to the Bartol96 predictions, thus favouring ν oscillations.

Table 1 gives the measured and expected events for the 3 topologies. They all favor ν oscillations. The L/E_ν distribution, Fig. 7a, deviates from MC expectations without oscillations; the deviations point to the same $\nu_\mu \longleftrightarrow \nu_\tau$ oscillation scenario [31] [34] [50].

$\nu_\mu \longleftrightarrow \nu_\tau$ against $\nu_\mu \longleftrightarrow \nu_{sterile}$. Matter effects due to the difference between the weak interaction effective potential for muon neutrinos with respect to sterile neutrinos, which have null potential, yield different total number and different zenith distributions of upthroughgoing muons [34]. The measured ratio R_{meas} between the events with $-1 < \cos \Theta < -0.7$ and with $-0.4 < \cos \Theta < 0$ was used [34]. In this ratio most of the theoretical uncertainties on neutrino flux and cross sections cancel (combining the experimental and theoretical errors in quadrature, a global uncertainty of 6% is obtained). The measured ratio is $R_{meas} = 1.38$, to be compared with $R_\tau = 1.61$ and $R_{sterile} = 2.03$. One

	Events	MC _{no osc} [61]	$R = \text{Data}/\text{MC}_{\text{no osc}}$
Upthr.	857	1169	0.73
IU	157	285	0.55
ID+UGS	262	375	0.70

Table 1: Summary of the MACRO $\nu_\mu \rightarrow \mu$ events in $-1 < \cos\theta < 0$ after background subtraction. For each topology (see Fig. 2) the number of measured events, the MC prediction for no-oscillations and the ratio (Data/MC-no osc) are given.

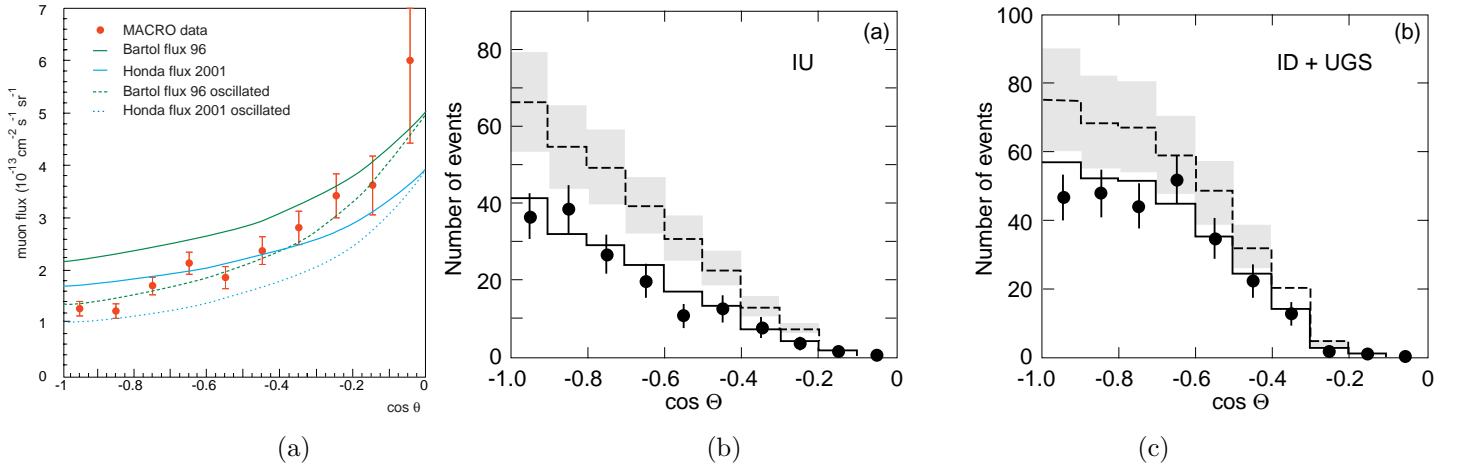


Figure 5: (a) Comparison between the zenith distribution of the MACRO upthroughgoing muons and the oscillated MC predictions given by Bartol96 (solid curve), HKKM01 (dash-dotted line), FLUKA fitted to the new CR measurements (dashed curve) and FLUKA with the old CR fit (dotted curve). Zenith distributions (b) for IU and (c) for ID+UGS events (black points) compared with the no oscillation Bartol96 MC (dashed line with a scale error band) and with the $\nu_\mu \longleftrightarrow \nu_\tau$ predictions with $\Delta m^2 = 2.3 \cdot 10^{-3} \text{ eV}^2$ and maximal mixing.

concludes that $\nu_\mu \longleftrightarrow \nu_{\text{sterile}}$ oscillations (with any mixing) are excluded at the 99.8% c.l. compared to the $\nu_\mu \longleftrightarrow \nu_\tau$ channel, see Fig. 6.

ν_μ energy estimate by Multiple Coulomb Scattering (MCS) of upthroughgoing muons. Since MACRO was not equipped with a magnet, the only way to estimate the muon energy was through their Multiple Coulomb Scattering (MCS) in the absorbers. Two analyses were performed [39] [46]. The first was made studying the deflection of muons using the streamer tubes in digital mode. This method had a spatial resolution of $\sim 1 \text{ cm}$. The second analysis was performed using the streamer tubes in “drift mode”. To check the electronics and the feasibility of the analysis two tests were performed at the CERN PS. The space resolution was $\simeq 3 \text{ mm}$. For each muon, 7 MCS variables were defined and given in input to a Neural Network, trained with MC events of known energy crossing the detector at different zenith angles. The output of this program gave the muon energy estimate event by event. The sample of upthroughgoing muons was separated in 4 subsamples with average energies E_μ of 12, 20, 50 and 100 GeV. The ratios $\text{Data}/\text{MC}_{\text{no osc}}$ as a function of $\log_{10}(L/E_\nu)$ for upthroughgoing muons are plotted in

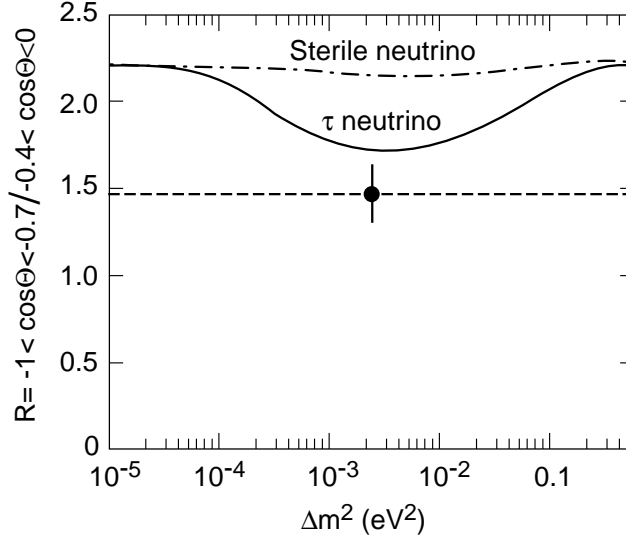


Figure 6: Ratio of events with $-1 < \cos\theta < -0.7$ to events with $-0.4 < \cos\theta < 0$ as a function of Δm^2 for maximal mixing. The black point with error bar is the measured value, the solid line is the prediction for $\nu_\mu \rightarrow \nu_\tau$ oscillations, the dash-dotted line is the prediction for $\nu_\mu \rightarrow \nu_{sterile}$ oscillations.

Fig. 7a; they are in agreement with the $\nu_\mu \longleftrightarrow \nu_\tau$ oscillation hypothesis [31] [34] [50].

New determination of the oscillation parameters. In the early analyses MACRO fitted the shape of the upthroughgoing muon zenith distribution and the absolute flux compared to Bartol96. This yielded $\Delta m^2 = 2.5 \cdot 10^{-3} \text{ eV}^2$ and maximal mixing [31] [34]. Later, in order to reduce the effects of systematic uncertainties in the MC simulations, MACRO used the following three independent ratios (it was checked that FLUKA, HKKM01 and Bartol96 MC yield the same predictions to within $\sim 5\%$):

- (i) High Energy Data: zenith distribution ratio: $R_1 = N_{vert}/N_{hor}$
- (ii) High Energy Data: ν energy measurement ratio: $R_2 = N_{low}/N_{high}$
- (iii) Low Energy Data: $R_3 = (Data/MC)_{IU}/(Data/MC)_{ID+UGS}$.

The no oscillation hypothesis has a probability $P \sim 3 \cdot 10^{-7}$ and is thus ruled out by $\sim 5\sigma$. By fitting the 3 ratios to the $\nu_\mu \longleftrightarrow \nu_\tau$ oscillation formulae, we obtained $\sin^2 2\theta = 1$, $\Delta m^2 = 2.3 \cdot 10^{-3} \text{ eV}^2$ and the allowed region indicated by the solid line in Fig. 7b. There is good consistency between the old and new methods [50]. Using Bartol96, it is possible to add the information on absolute fluxes:

- (iv) High energy data (systematic error $\simeq 17\%$): $R_4 = N_{meas}/N_{MC}$.
- (v) Low energy semicontained muons (scale error 21%): $R_5 = N_{meas}/N_{MC}$.

These informations leave the best fit values unchanged and reduce the area of the allowed region, as indicated by the dashed line in Fig. 7b. (6σ significance).

Fig. 8 shows one page of the 1984 proposal [1]. It stated that MACRO could yield valuable information on possible neutrino oscillations in the then unexplored region indicated by the shaded area: in fact atmospheric neutrino oscillations were found there! [67].

Exotic oscillations. MACRO and SuperK data have been used to search for subdominant oscillations due to possible Lorentz invariance violation (or violation of the equivalence principle). In the first case there could be mixing between flavor and velocity

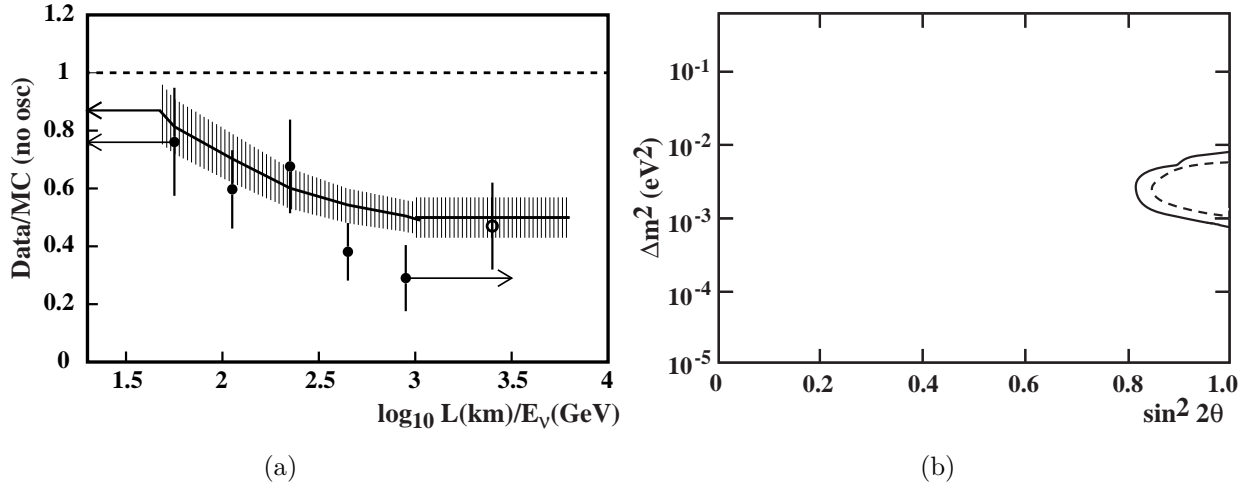


Figure 7: (a) Data/MC_{no osc} vs L/E_ν for upthroughgoing muons (black points). The solid line is the MC expectation for $\Delta m^2 = 2.3 \cdot 10^{-3} \text{ eV}^2$ and $\sin^2 2\theta = 1$. The last point (empty circle) is obtained from the IU sample. (b) Interpolated 90% c.l. contour plots of the allowed regions in the $\Delta m^2 - \sin^2 2\theta$ plane for the MACRO data using only the ratios R_1, R_2, R_3 (continuous line) and adding also the information on the absolute values R_4, R_5 (dotted line).

Hence, in two years of operation, our experiment can set a 3σ limit for neutrino oscillations for mass differences in excess of 10^{-3} eV^2 for maximal mixing. In Fig. (2)13, this limit (shaded region) is compared with the present limits set by other neutrino oscillation experiments. For $\sin^2 2\theta > 0.6$, the experiment should yield nearly an order of magnitude improvement for the limit on Δm^2 .

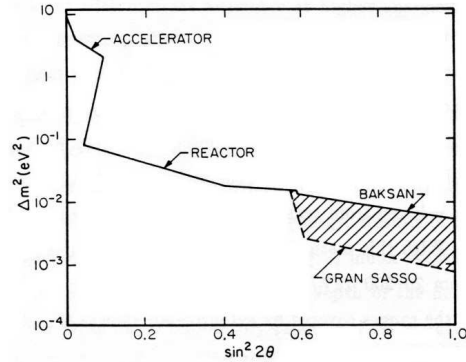


Fig. (2)13 Present best limits on Δm^2 vs. $\sin^2 2\theta$. The shaded region represents the improvement obtainable with our experiment.

Figure 8: From the 1984 MACRO proposal [1].

eigenstates. The data disfavor these exotic possibilities, even at a sub-dominant level. Stringent 90% c.l. limits were placed in the Lorentz invariance violation parameters $|\Delta v| < 6 \cdot 10^{-24}$ at $\sin^2 2\theta_v=0$ and $|\Delta v| < 4 \cdot 10^{-26}$ at $\sin^2 2\theta_v = \pm 1$ [68] [69].

Neutrino decay. It could be another exotic partial explanation for neutrino disappearance; no radiative decay has been observed [70].

4 Search for Astrophysical Point Sources of HE ν_μ 's

High energy ν_μ 's are expected to come from several galactic and extragalactic sources. Neutrino production requires astrophysical accelerators of charged particles and astrophysical beam dumps. The good angular resolution of MACRO allowed a sensitive search for upgoing muons produced by neutrinos coming from celestial sources, with a negligible atmospheric neutrino background. An excess of events was searched for around the positions of known sources in 3° (half width) angular bins. This value was chosen to take into account the angular smearing produced by the multiple muon scattering in the rock below the detector and by the energy-integrated angular distribution of the scattered muon with respect to the neutrino direction. In a total livetime of 6.16 y we obtained 1356 events, Fig. 9. The 90% c.l. upper limits on the muon fluxes from specific celestial sources lay in the range $10^{-15} - 10^{-14} \text{ cm}^{-2} \text{ s}^{-1}$, Fig. 9b. The solid line is MACRO sensitivity vs. declination. Notice the two cases, GX339-4 ($\alpha = 255.71^\circ$, $\delta = -48.79^\circ$) and Cir X-1 ($\alpha = 230.17^\circ$, $\delta = -57.17^\circ$), with 7 events: in Fig. 9 they are considered as background, thus the upper flux limits are higher; but they could also be indications of signals [33].

We searched for time coincidences of our upgoing muons with γ -ray bursts as given in the BATSE 3B and 4B catalogues, for the period from 1991-2000 [33]. No statistically significant time correlation was found.

We have also searched for a diffuse astrophysical neutrino flux for which we establish a flux upper limit at the level of $1.5 \cdot 10^{-14} \text{ cm}^{-2} \text{ s}^{-1}$ [37].

5 Indirect Searches for WIMPs

Weakly Interacting Massive Particles (WIMPs) may be part of the galactic dark matter; they may be intercepted by celestial bodies, slowed down and trapped in their centers, where WIMP and anti-WIMP could annihilate yielding upthoroughgoing muons. The annihilations yield ν_μ of GeV energy, in small angular windows from their centers.

For the Earth we have chosen a 15° cone around the vertical: we found 863 events. The MC expectation for atmospheric ν_μ without oscillations gave a larger number of events. We set a conservative flux upper limit assuming that the measured number of events equals the expected ones. The 90% c.l. limits for the flux of upgoing muons are shown in Fig. 10a (it varies from about 0.8 to $0.5 \cdot 10^{-14} \text{ cm}^{-2} \text{ s}^{-1}$). If the WIMPs are identified with the smallest mass neutralino, the MACRO limit may be used to constrain the stable neutralino mass, following the model of Bottino et al. [71] [28], see Fig. 10a.

A similar procedure was used to search for ν_μ from the Sun, using 10 search cones. In the absence of statistically significant excesses muon upper limits at the level of $1.5 - 2 \cdot 10^{-14} \text{ cm}^{-2} \text{ s}^{-1}$ were established, see Fig. 10b.

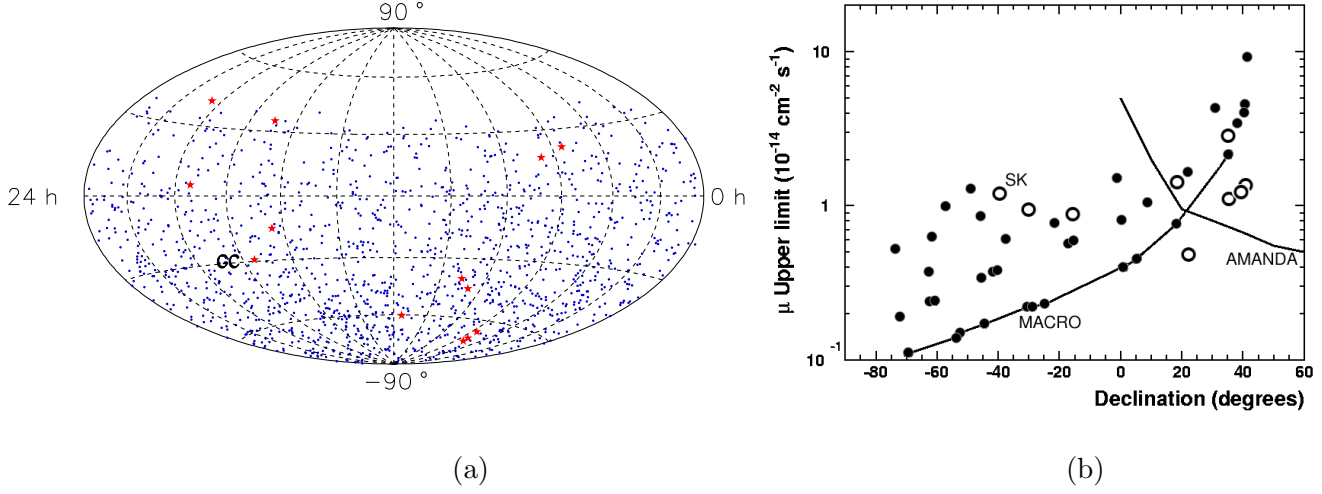


Figure 9: High energy neutrino astronomy. (a) Upgoing muon distribution in equatorial coordinates (1356 events). (b) The black points are the MACRO 90 % c.l. upgoing muon flux limits vs declination for 42 selected point sources. The solid line refers to the limits obtained for those cases for which the atmospheric neutrino background was zero. The limits from the SK (open circles) and AMANDA (thin line) experiments are quoted; these limits refer to higher E_ν .

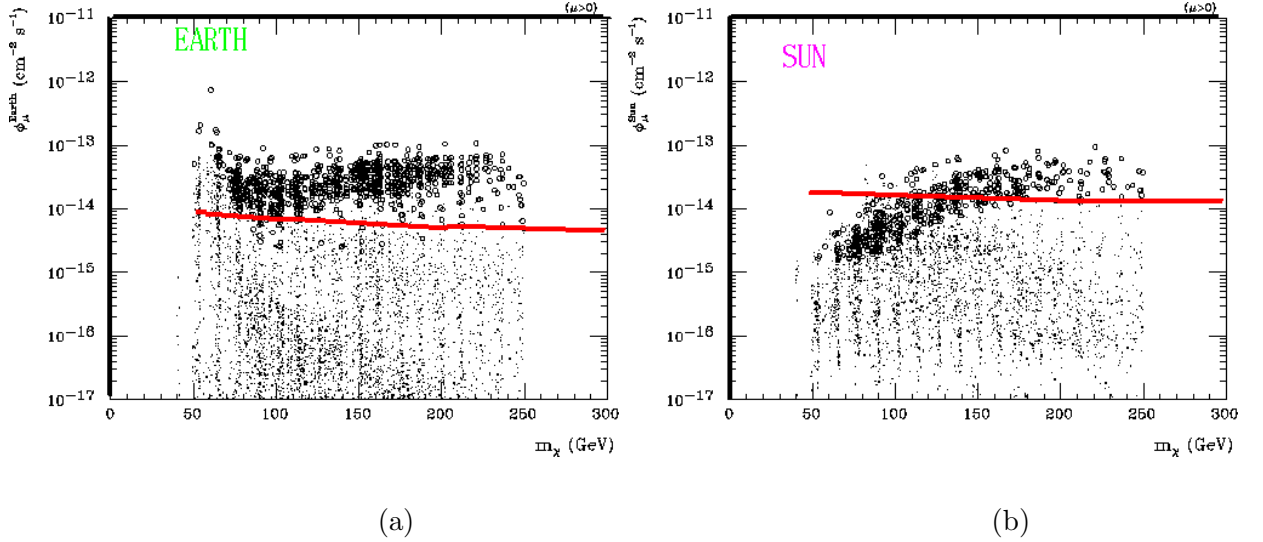


Figure 10: (a) The solid line is our upwardgoing muon flux upper limit (90% c.l.) from the Earth plotted vs. neutralino mass m_χ ($E_\mu^{th}=1 \text{ GeV}$). (b) As in (a) but for upwardgoing muons from the Sun [28]. Each dot is obtained varying model parameters. The open circles indicate models *excluded* by direct measurements, assuming a local dark matter density of $\sim 0.5 \text{ GeV cm}^{-3}$.

6 Magnetic Monopoles and Nuclearites

The concept of magnetic monopole (MM) may be traced back to the origin of magnetism. In 1931 Dirac introduced MMs in order to explain the quantization of the electric charge, obtaining the formula $eg = n\hbar c/2$, from which $g = ng_D = n\hbar c/2 = n3.29 \cdot 10^{-8}$ c.g.s.; n is an integer [72].

Supermassive monopoles predicted by Grand Unified Theories (GUT) of the electroweak and strong interactions should have masses of the order of $m_M \sim 10^{17}$ GeV [73]. These MMs could be present in the penetrating cosmic radiation and are expected to arrive isotropically from all directions and to have typical galactic velocities, $\sim 10^{-3}c$, if trapped in our Galaxy. MMs trapped in our solar system or in the supercluster of galaxies may travel with typical velocities of the order of $\sim 10^{-4}c$ and $\sim 10^{-2}c$, respectively [74].

The search for GUT magnetic monopoles was one of the main objectives of MACRO.

Monopoles, in the presence of strong magnetic fields, may reach higher velocities. Possible Intermediate Mass MMs could achieve relativistic velocities, but they could reach MACRO only from above.

The reference sensitivity level for a significant MM search is the Parker bound [74], the maximum monopole flux compatible with the survival of the galactic magnetic field. This limit is of the order of $\Phi \lesssim 10^{-15} \text{ cm}^{-2} \text{ s}^{-1} \text{ sr}^{-1}$, but it could be reduced by almost an order of magnitude when considering the survival of a small galactic magnetic field seed. Our experiment was designed to reach a flux sensitivity for GUT MMs well below the Parker bound, in the MM velocity range $4 \times 10^{-5} < \beta < 1$. The three MACRO sub-detectors had sensitivities in wide β -ranges, with overlapping regions; thus they allowed multiple signatures of the same rare event candidate.

No candidate was found in many years of data taking by any of the three subdetectors. The MM flux limits set by different analyses using the three subdetectors over different β -range were combined to obtain a global MACRO limit. For each β value, the global time integrated acceptance was computed as the sum of the independent portions of each analysis. The limits versus β are shown in Fig. 11 together with the limits set by other experiments [74, 86, 87]; other limits are quoted in [40]. The limits obtained with the MACRO NTDs only are shown in Fig. 11b: our limits are the best direct limits existing for GUT MMs over a wide range of β , $4 \times 10^{-5} < \beta < 1$; see ref. [75] [76] for stringent limits with indirect experiments. Energy losses are computed in ref. [67] [77].

A specific search for GUT monopole catalysis of nucleon decay was made with our streamer tube system. Since no event was found, one can place a monopole flux upper limit at the level of $\sim 3 \cdot 10^{-16} \text{ cm}^{-2} \text{ s}^{-1} \text{ sr}^{-1}$ for $10^{-4} \lesssim \beta \lesssim 5 \cdot 10^{-3}$, valid for a large catalysis cross section, $5 \cdot 10^2 < \sigma_{cat} < 10^3 \text{ mb}$ [41]. The flux limit for the standard direct MM search with streamer tubes is valid for $\sigma_{cat} < 100 \text{ mb}$.

The MM searches based on the scintillator and on the nuclear track subdetectors were also used to set new upper limits on the flux of cosmic ray *nuclearites* (strange quark matter), over the same β range. If nuclearites are part of the dark matter in our galaxy, the most interesting β is of the order of $\sim 10^{-3}$ [78]. Some of the nuclearite limits apply also to charged *Q-balls* (agglomerates of squarks, sleptons and Higgs fields and other objects) [79][80][88].

The energy losses of MMs, dyons and of other heavy particles in the Earth and in different detectors for various particle masses and velocities were computed in [77].

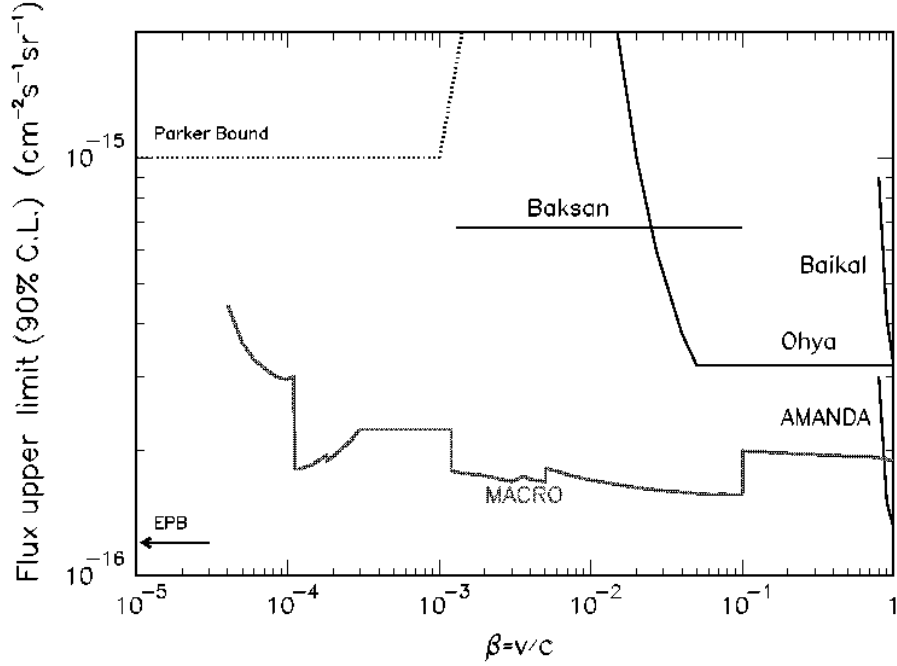


Figure 11: (a) Magnetic monopole flux upper limits at the 90% c.l. obtained by MACRO and by other experiments. The limits apply to singly charged ($g = g_D$) monopoles assuming that catalysis cross sections are smaller than a few mb. (b) Limits obtained with the MACRO NTDs only, for GUT monopoles with $g = g_D, 2g_D, 3g_D$ and for dyons.

7 Neutrinos from Stellar Gravitational Collapses

A stellar gravitational collapse (GC) of the core of a massive star is expected to produce a burst of all types of ν and $\bar{\nu}$ with energies of 7 – 30 MeV and a duration of 10 s. The $\bar{\nu}_e$'s can be detected via the process $\bar{\nu}_e + p \rightarrow n + e^+$ in liquid scintillators; $100 \div 150$ $\bar{\nu}_e$ events were expected in our scintillator for a stellar collapse at the center of our Galaxy.

We used two electronic systems for detecting $\bar{\nu}_e$'s from stellar gravitational collapses. The first system was based on the dedicated PHRASE trigger, the second one was based on the ERP trigger, see sect. 2. Both systems had an energy threshold of ~ 7 MeV and recorded pulse shape, charge and timing informations. Immediately after a > 7 MeV trigger, the PHRASE system lowered its threshold to about 1 MeV, for $800 \mu s$, to detect (with a $\simeq 25\%$ efficiency) the 2.2 MeV γ released in the reaction $n + p \rightarrow d + \gamma_{2.2 \text{ MeV}}$ induced by the neutron produced in the primary process.

A redundant supernova alarm system was in operation, alerting immediately the physicists on shift. We defined a general procedure to alert the physics and astrophysics communities in case of an interesting alarm. Finally, a procedure to link the various supernova observatories around the world was set up [23].

The effective MACRO active mass was ~ 580 t; the live-time fraction in the last four years was $\simeq 97.5\%$. No stellar gravitational collapse was observed in our Galaxy from the beginning of 1989 to the end of 2000 [45].

8 Cosmic Ray Muons

MACRO large area and acceptance allowed to record $6 \cdot 10^7$ single muons, $3.7 \cdot 10^6$ multiple muons and to study many aspects of physics and astrophysics of cosmic rays (CR).

Muon vertical intensity. The underground muon vertical intensity vs rock thickness gives information on the high energy ($E \gtrsim 1.3$ TeV) atmospheric muon flux and on the all-particle primary CR spectrum. The results constrain the CR production and interaction models. A study performed in 1995 covered the overburden range $2200 \div 7000$ hg/cm² [16].

Analysis of high multiplicity muon bundles. The **multiplicity distribution** of muon bundles provides information on the primary CR composition model. The **decoherence** function (the distribution of the distance between two muons in a muon bundle) gives information on the hadronic interaction features at high energies; a study was performed using a large sample of data and improved MC methods, Fig. 12a [29]. Different hadronic interaction models (DPMJET, QGSJET, SIBYLL, HEMAS, HDPM) interfaced to the HEMAS and CORSIKA shower propagation codes were used.

Muon correlations inside a bundle were studied, using the so called correlation integral [88], to search for dynamical correlations in the bundles. Since the cascade development in atmosphere is mainly determined by the number of “steps” in the “tree formation”, we expect a different behaviour for cascades originated by light and heavy CR primaries. For the same reason, the analysis is less sensitive to the hadronic interaction model used in the simulations. For $E_{pr} > 1000$ TeV, the composition model derived from the analysis of the muon multiplicity distribution [19, 20] is almost independent of the interaction model.

We also searched for *substructures (“clusters”) inside muon bundles* [82]. The search was performed by means of different software algorithms; the study is sensitive to both hadronic interaction and primary CR composition models. If the primary composition has been determined by the first method, a choice of the bundle topology gives interesting connections with the early hadronic interaction features in the atmosphere. The comparison between our data and MC simulations allowed to place constraints on the interaction models. The same MC study has shown that muon bundles with a central core and an isolated cluster with at least two muons are the result of random associations. An analysis of the decoherence function for high multiplicity events has shown that QGSJET is the hadronic interaction model which better reproduces the underground observables.

The ratio double muons/single muons: The ratio N_2/N_1 of double muon over single muon events is expected to decrease at increasing rock depths. The LVD collaboration reported an increase of the ratio multiple-muons to all-muons for rock depths $h > 7000$ hg/cm². We measured the ratio as a function of the rock depth, using also multiple muon events at large zenith angles. A detailed MC simulation was made using the HEMAS code, with the zenith angle extended up to 89°. The event direction was reconstructed by the tracking system. The rock depth is provided by the Gran Sasso map function $h(\theta, \phi)$ up to $\theta = 94^\circ$. MC simulations have shown that the percentage of events with mis-reconstructed multiplicity is $< 3\%$. Attention was devoted to “cleaning” the events from spurious effects; we also made a visual scanning of the events. Our measured ratios N_2/N_1 as a function of the rock depth, Fig. 12(b), are in agreement with the expectation of a monotonic decrease up to ~ 10000 hg/cm². Above this value, the low statistics does not allow a firm conclusion on a possible increase of N_2/N_1 [82].

Muon Astronomy [68]. Some past experiments reported excesses of a modulated muon

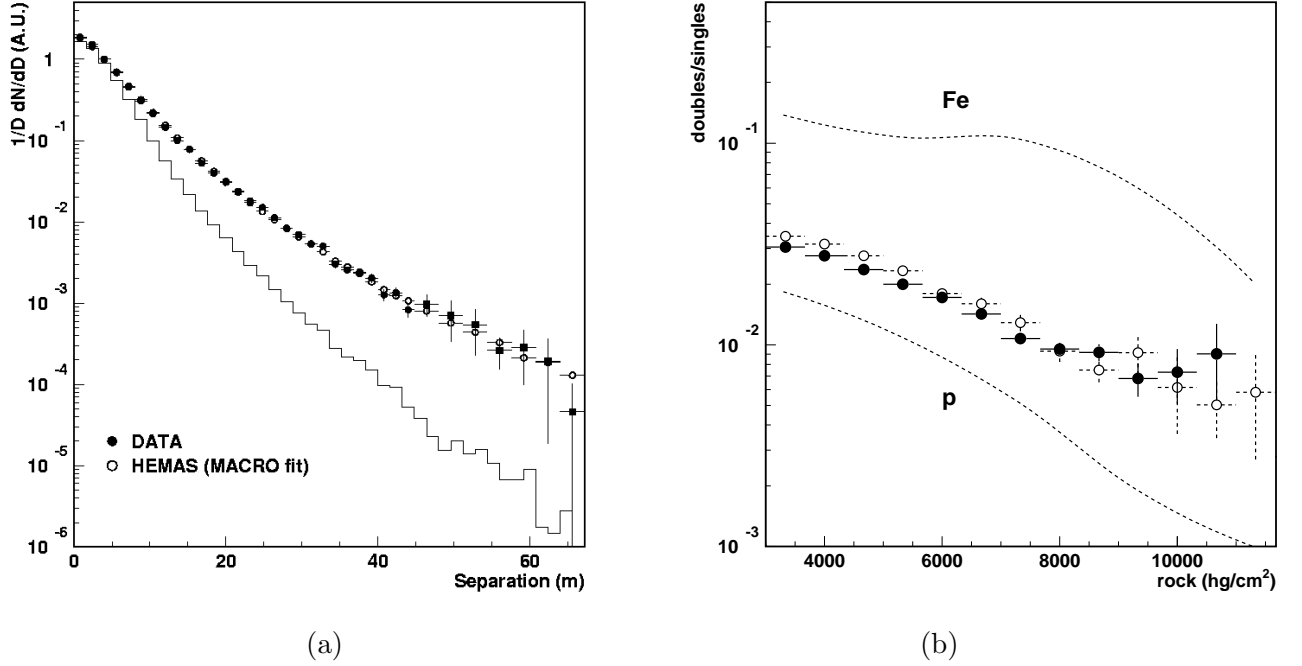


Figure 12: (a) Unfolded experimental decoherence distribution for an infinite detector (black points) compared with MC expectations (open points); the histogram is the measured decoherence distribution before unfolding [29]. (b) Ratio of double to single muon events vs the rock depth. The black points are our data; the open circles are MC predictions made using the MACRO composition model. The dashed lines are MC predictions using pure proton and iron primaries.

flux from the direction of Cyg X-3. Our data did not indicate excesses above background, both for steady dc fluxes and for modulated ac fluxes. Our pointing precision was checked via the shadow of the Moon and of the Sun on primary CRs. The pointing resolution was checked with double muons. The angle containing 68% of the events in a $\Delta\theta$ bin was 0.8° . *All sky d.c. survey.* The sky, in galactic coordinates, was divided into bins of equal solid angle, $\Delta\alpha = 3^\circ$, $\Delta\sin\delta = 0.04$, corresponding to cones of 1.5° half angles. In order to remove edge effects, three other surveys were done, by shifting the map by one-half bin in α , by one-half bin in $\sin\delta$ and with both α and $\sin\delta$ shifted. For each solid angle bin we computed the deviation from the average muon intensity, after background subtraction. No deviation was found; the 95% flux upper limits were $\leq 5 \times 10^{-13} \text{cm}^{-2} \text{s}^{-1}$.

Specific point-like d.c. sources. For Cyg X-3, Mrk421, Mrk501 we searched in a narrow cone (1° half angle) around the source direction. We obtained flux limits at the level of $(2 - 4) \cdot 10^{-13} \text{cm}^{-2} \text{s}^{-1}$. There is a small excess of 2.0σ in the direction of Mrk501.

Modulated a.c. search from Cyg X-3 and Her X-1. No evidence for an excess was observed and the limits are $\Phi < 2 \times 10^{-13} \text{cm}^{-2} \text{s}^{-1}$, see Fig. 13.

Search for bursting episodes. A search was made for pulsed muon signals in a 1° half angle cone around the location of high energy photon sources. Bursting episodes of duration of ~ 1 day were searched for with two different methods. In the first we searched for daily excesses of muons above the background, also plotting cumulative excesses day by day. In the second method we computed day by day the quantity $-\text{Log}_{10}P$ where P is the probability to observe a burst at least as large as N_{obs} . We find some possible excesses for Mrk421 on the days 7/1/93, 14/2/95, 27/8/97, 5/12/98.

Seasonal variations. Underground muons are produced by mesons decaying in flight in

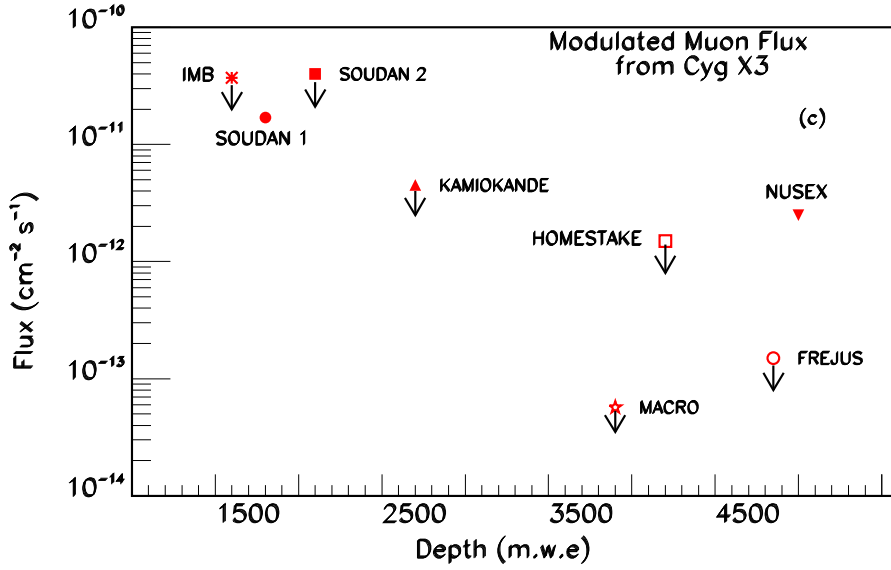


Figure 13: Searches for a modulated muon signal from Cyg X-3. The Soudan 1 and Nusex collaborations reported positive indications, while other experiments give flux upper limits.

the atmosphere. The muon flux thus depends on the ratio between decay and interaction probabilities of the parent mesons, which are sensitive to the atmospheric density and temperature. The flux decreases in winter, when the temperature is lower and the atmosphere more dense, and increases in summer; the variations are of $\pm 2\%$, Fig. 14.

Solar daily variations. Because of changes in the day-night temperatures we expect solar daily variations similar to seasonal variations, but of smaller amplitudes. These variations were found with an amplitude $A = (0.88 \pm 0.26) \cdot 10^{-3}$ at a significance of 3.4σ , Fig. 15a.

Sidereal anisotropies are due to the motion of the solar system in the “sea” of relativistic cosmic rays in our galaxy. They are expected to yield a small effect. After a correction due to the motion of the Earth around the Sun, we observed variations with an amplitude $8.6 \cdot 10^{-4}$ and a phase $\phi_{max} = 22.7^\circ$ with a statistical significance of 3σ , Fig. 15b.

Moon and sun shadows of primary cosmic rays. The pointing capability of MACRO was demonstrated by the observed “shadows” of the Moon and of the Sun. A sample of $45 \cdot 10^6$ muons was used to look at the bidimensional density of the events around the directions of the Moon and of the Sun, Fig. 16. For the Moon: we looked for events in a window $4.375^\circ \times 4.375^\circ$ centered on the Moon; the window was divided into 35×35 cells, each of dimensions $0.125^\circ \times 0.125^\circ$ ($\Delta\Omega = 1.6 \cdot 10^{-2} \text{deg}^2$); Fig. 16a shows a depletion of events with a statistical significance of 5.5σ . The observed slight displacement of the maximum deficit is consistent with the displacement of the primary protons due to the geomagnetic field. The same analysis was repeated for muons in the sun window, Fig. 16b. The difference between the apparent sun position and the observed muon depletion is due to the combined effect of the magnetic field of the Sun and of the Earth. The observed depletion has a statistical significance of 4.5σ [44][26].

Muon energy measurement with the TRD detector. The underground differential energy spectrum of muons was measured with the TRD detector. Two types of events were analyzed: “single muons”, i.e. single muons in MACRO crossing a TRD module,

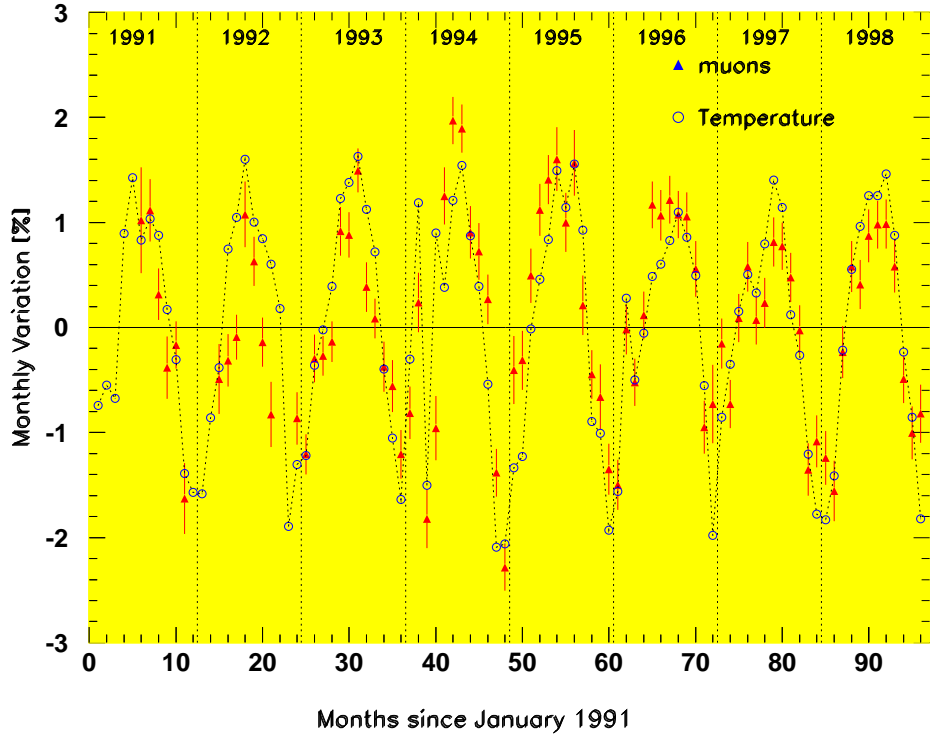
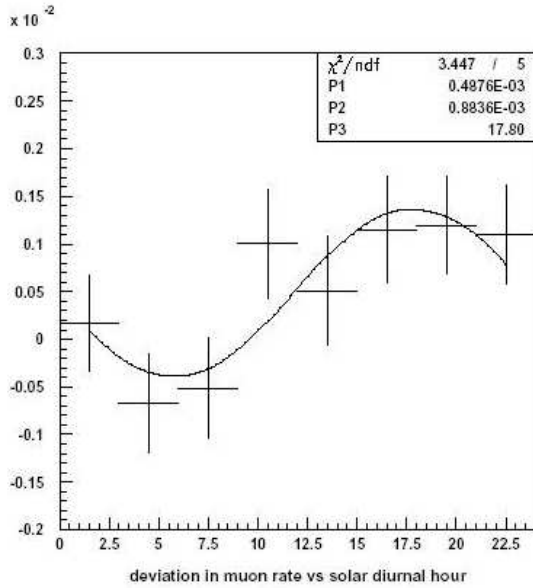
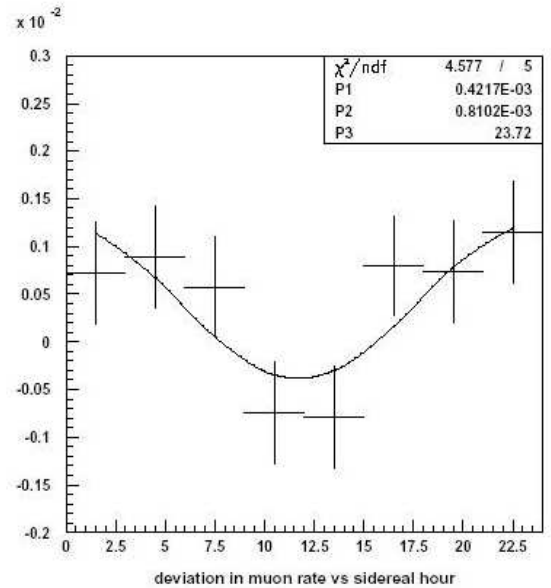


Figure 14: Seasonal variation of the muon flux from above (black triangles); the open circles are measurements of the temperature of the upper atmosphere.



(a)



(b)

Figure 15: Deviations of the muon rate from the mean muon rate (a) versus the local solar diurnal time at Gran Sasso, and (b) versus the local sidereal time.

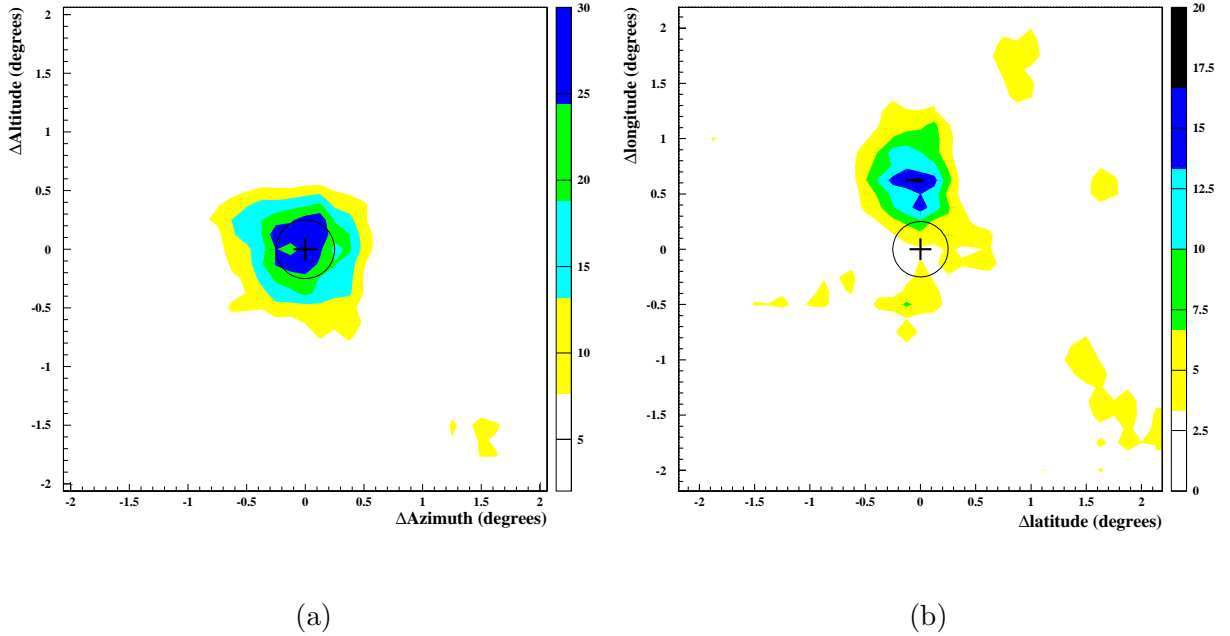


Figure 16: Moon and sun shadows. (a) Two dimensional distributions of muon event density around the moon direction. The regions of increasing gray scale indicate increasing levels of deficit in percent. (b) Same analysis for the sun direction.

and “double muons” in MACRO with only one muon crossing the TRD detector. The measurements refer to muons with energies $0.1 < E_\mu < 1 \text{ TeV}$ and for $E_\mu > 1 \text{ TeV}$ [27][42]. In order to evaluate the local muon energy spectrum, we took into account the TRD response function. The average single muon energy in the underground lab is 270 GeV; for double muons is 380 GeV.

9 EAS-TOP/MACRO Coincidences

For coincident events, the Extensive Air Showers EASTOP measured the e.m. size of the showers at Campo Imperatore, while MACRO measured muons underground. The purpose was the study of primary CR composition vs energy reducing the dependence on the interaction and propagation models. The two detectors operated in coincidence for a livetime of 960 days. The number of coincident events was 28160, of which 3752 had shower cores inside the edges of EASTOP (“internal events”) and shower sizes $N_e > 2 \cdot 10^5$; 409 events had $N_e > 10^{5.92}$, i.e. above the CR knee. The data were analyzed in terms of the QGSJET interaction model implemented in CORSIKA [14][47][48][84].

The e.m. detector of EASTOP covered an effective area of 10^5 m^2 . The array was fully efficient for $N_e > 10^5$. The reconstruction capabilities of the air shower parameters for internal events were: $\frac{\Delta N_e}{N_e} \simeq 10\%$ for $N_e \gtrsim 10^5$, and $\Delta\theta \sim 0.9^\circ$ for the arrival direction. MACRO considered muons with ≥ 4 aligned hits in both views of the horizontal streamer tube planes. Inside the EASTOP effective area, the muon energy threshold at the surface, for muons reaching MACRO, ranged from 1.3 to 1.8 TeV. Coincidences were made off-line, using the absolute time given by a GPS system with an accuracy $\leq 1 \mu\text{s}$.

The data considered were the muon multiplicity distributions in different intervals of

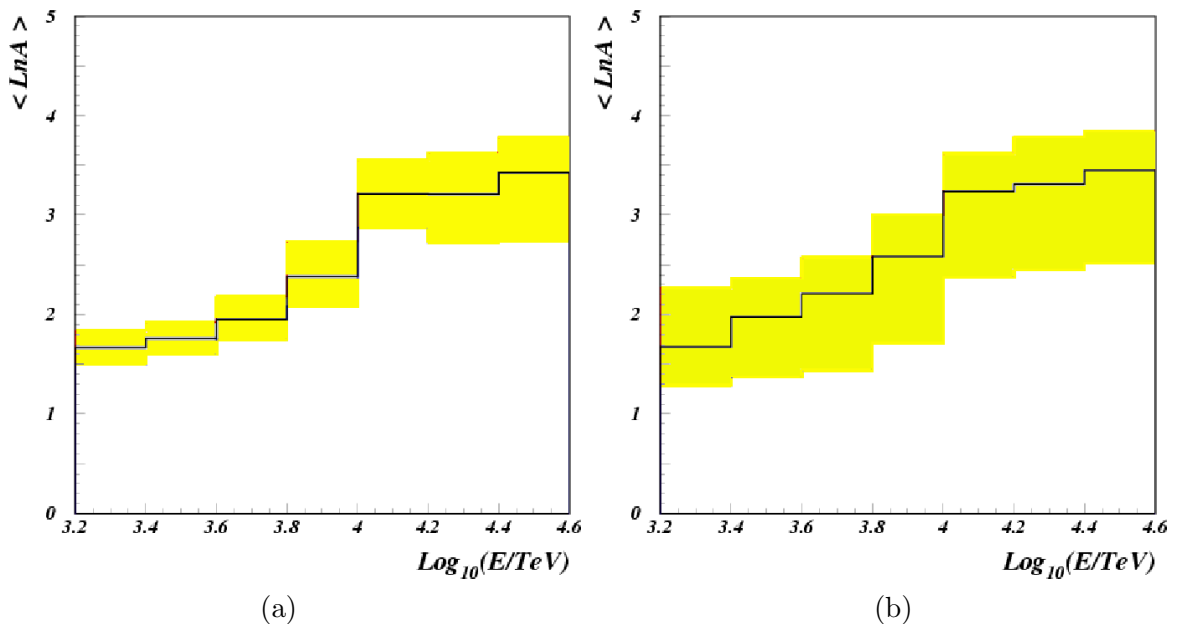


Figure 17: EASTOP-MACRO coincidences. $\langle \ln A \rangle$ vs primary energy for: (a) p/Fe and (b) $Light/Heavy$ compositions. The (black lines) are the data, the shaded areas indicate the uncertainties discussed in the text.

shower sizes. For each bin the muon distribution was fitted with a superposition of (i) pure p and Fe components, or (ii) light (L) and heavy (H) admixtures containing equal fractions of p and He or Mg and Fe , respectively. All spectra in the simulation have slope $\gamma = 2.62$. In each interval a χ^2 expression was minimized.

Fig. 17 shows $\langle \ln A \rangle$ vs $\log_{10} E$ (E in TeV); the shaded regions include the uncertainties for (a) the p/Fe composition model and (b) for the light/heavy model. There is an increase of $\langle \ln A \rangle$ with energy in the CR knee region.

The coincidences allowed to measure the lateral distribution of Cherenkov light collected by EASTOP in the $10 \div 100$ TeV range associating it with the TeV muon in MACRO. The test provided a validation of the CORSIKA-QGSJET code [84].

10 Nuclear Track Detector Calibrations

Many calibrations of the CR39 nuclear track detector (NTD) were performed with both slow and fast ions. In all measurements we have seen no deviation of its response from the Restricted Energy Loss (REL) model. Stacks of CR39 and Lexan foils, placed before and after various targets, were exposed to 158 A GeV Pb^{82+} ions at the CERN-SPS and to 1 A GeV Fe^{26+} ions at the BNL-AGS. In traversing a target, the beam ions produce nuclear fragments with $Z < 82$ and $Z < 26$ for the lead and iron beams, respectively; this allows a measurement of the response of the detector in a Z region relevant to MM detection. Previous analyses had shown that the CR39 charge resolution for a single measurement is $0.19e$ in the range $72 \leq Z \leq 83$ (by measurements of the etch-cone heights); at lower Z the measurements of the cone base diameters allow to separate the different charges. Tests were made looking for a possible aging effect, from the time elapsed from the production

date to the exposure date [85]. Two sets of sheets, 0.8 y and 2.5 y old, were exposed in 1994 to 158 A GeV Pb^{82+} ions. For each detected nuclear fragment the reduced etch rate $p = v_T/v_B$ (v_T and v_B are the track and bulk etching rates) was computed and plotted vs REL. Within the experimental uncertainties, aging effects in the CR39 are negligible.

11 Search for Lightly Ionizing Particles

Free fractionally charged particles could be expected in Grand Unified Theories; the expected charges range from $Q=e/5$ to $Q=e/2$. They should release a fraction $(Q/e)^2$ of the energy deposited by a relativistic muon traversing a medium. Lightly Ionizing Particles (LIPs) were searched for in MACRO using a four-fold coincidence between three layers of scintillators and the streamer tube system [32][49]. The 90 % c.l. flux upper limits for LIPs with charges $2e/3$, $e/3$ and $e/5$ are at the level of $1.5 \cdot 10^{-15} cm^{-2} s^{-1} sr^{-1}$.

12 Conclusions

MACRO obtained important results in all the items listed in the proposal :

- *GUT Magnetic Monopoles*. We obtained the best flux upper limit over the widest β range, thanks to the large acceptance and the redundancy of the different techniques employed. This limit is a unique result and it will stand for a long time.
- *Atmospheric neutrino oscillations*. In this field MACRO had its major achievements. Analyses of different event topologies, different energies and the exploitation of Coulomb multiple scattering in the detector strongly support $\nu_\mu \rightarrow \nu_\tau$ oscillations.
- *High energy ν_μ astronomy*. Our detector was competitive with other underground/underwater experiments thanks to its good angular accuracy.
- *Search for bursts of $\bar{\nu}_e$ from stellar gravitational collapses*. MACRO was sensitive to supernovae events in the Galaxy, it started the SN WATCH system, and for a period it was the only detector in operation.
- *Cosmic ray downgoing muons*. We observed the shadows of primary CRs by the Moon and the Sun, the seasonal variation ($\sim 2\%$ amplitude) over many years, solar and sidereal variations with reasonable statistical significances. No excesses of secondary muons attributable to astrophysical point sources (steady, modulated or bursting) were observed.
- Exploration of the *CR composition* around the “knee” of the primary CR energy.
- *Coincidences between MACRO and the EASTOP array*. The data indicate an increase with increasing energy of the average Z of the primary CR nuclei.
- Sensitive searches for exotic particles were carried out: (i) *WIMPs*, looking for upgoing muons from the center of the Earth and of the Sun; (ii) *Nuclearites* and *Q-balls* (as byproducts of MM searches). (iii) Other limits concern possible *Lightly Ionizing Particles*.

The dismantling of MACRO went regularly and essentially on schedule. We recuperated part of the electronics (modules, circuits, cables, etc) to be used in our Institutions, and donated the photomultipliers and part of the streamer tubes to other experiments.

The MACRO scientific and technical results were published in 50 papers in refereed journals, in 242 contributions to conferences and in invited papers, discussed in 543 Internal Memos, used for 83 italian Laurea theses, 22 italian Dottorato theses, 23 US PhD theses and 5 moroccan theses de Doctorat Nationale.

Acknowledgments

We thank all our colleagues for their cooperation, and wish all the best to Charles Peck. MACRO acknowledged the support of the Directors and of the staff of the Gran Sasso Lab. and of the Institutions participating in the experiment, the Istituto Nazionale di Fisica Nucleare (INFN), the US Department of Energy and the US National Science Foundation. INFN-FAI, ICTP (Trieste), NATO and WorldLab provided fellowships and grants for non-Italian citizens.

References

- [1] Proposal for a large area detector dedicated to monopole searches, astrophysics and cosmic ray physics at the Gran Sasso Lab., LNF preprint, July 10, 1984; CALT-68-1237, Nov.1984. C. De Marzo et al., Nuovo Cimento 9C(1986)281.
- [2] M.Calicchio et al., Nucl. Instr. Meth. Phys. Res. A264(1988)18.
- [3] R.Bellotti et al. Phys. Rev. D42(1990)1396.
- [4] S.Ahlen et al., Phys. Lett. B249(1990)149.
- [5] S.Ahlen et al., Nucl. Phys. B370(1992)432.
- [6] S.Ahlen et al., Phys. Rev. D46(1992)895.
- [7] S.Ahlen et al., Phys. Rev. D46(1992)4836.
- [8] S.Ahlen et al., Astropart. Phys. 1(1992)11.
- [9] S.Ahlen et al., Phys. Rev. Lett. 69(1992)1860.
- [10] S.Ahlen et al., Nucl. Instr. Meth. Phys. Res. A324(1993)337.
- [11] S.Ahlen et al., Astrophys. J. 412(1993)301.
- [12] S.Ahlen et al., Phys. Rev. Lett. 72(1994)608.
- [13] GRACE-MACRO Coll., M.Ambrosio et al., Phys. Rev. D50(1994)3046.
- [14] EASTOP-MACRO Coll., M.Aglietta et al., Phys. Lett. B337(1994)376.
- [15] M.Ambrosio et al., Astropart. Phys. 4(1995)33.
- [16] M.Ambrosio et al., Phys. Rev. D52(1995)3793.
- [17] S.Ahlen et al., Phys. Lett. B357(1995)481.
- [18] M.Ambrosio et al., Astropart. Phys. 6(1997)113.
- [19] M.Ambrosio et al., Phys. Rev. D56(1997)1407.
- [20] M.Ambrosio et al., Phys. Rev. D56(1997)1418.
- [21] M.Ambrosio et al., Astropart. Phys. 7(1997)109.
- [22] M.Ambrosio et al., Phys. Lett. B406(1997)249.
- [23] M.Ambrosio et al., Astropart. Phys. 8(1998)123.
- [24] M.Ambrosio et al., Astropart. Phys. 9(1998)105, hep-ex/9807032.
- [25] M.Ambrosio et al., Phys. Lett. B434(1998)451, hep-ex/9807005.
- [26] M.Ambrosio et al., Phys. Rev. D59(1999)012003, hep-ex/9807006.
- [27] M.Ambrosio et al., Astropart. Phys. 10(1999)11, hep-ex/9807009.
- [28] M.Ambrosio et al., Phys. Rev. D60(1999)082002, hep-ex/9812020.
- [29] M.Ambrosio et al., Phys. Rev. D60(1999)032001, hep-ex/9901027.
- [30] M.Ambrosio et al., Eur. Phys. J. C13(2000)453, hep-ex/9904031.
- [31] M.Ambrosio et al., Phys. Lett. B478(2000)5, hep-ex/0001044.
- [32] M. Ambrosio et al., Phys. Rev. D62(2000)052003, hep-ex/0002029.
- [33] M. Ambrosio et al., Astrophys. J. 546(2001)1038, astro-ph/0002492.
- [34] M.Ambrosio et al., Phys. Lett. B517(2001)59, hep-ex/0106049.
- [35] M.Ambrosio et al., Nucl. Instr. Meth. Phys. Res. A486(2002)663.
- [36] M.Ambrosio et al., Astropart. Phys. 18(2002)27, hep-ex/0110083.
- [37] M.Ambrosio et al., Astropart. Phys. 19 (2003)1, astro-ph/0203181.
- [38] M.Ambrosio et al., Astropart. Phys. 18 (2003) 615, hep-ph/0204188.
- [39] M.Ambrosio et al., Nucl. Instr. Meth. Phys. Res. A492 (2002)376, physics/0203018.

- [40] M.Ambrosio et al., Eur. Phys. J. C25 (2002) 511, hep-ex/0207020.
- [41] M.Ambrosio et al., Eur. Phys. J. C26 (2002) 163, hep-ex/0207024.
- [42] M.Ambrosio et al., Astropart. Phys. 19 (2003) 313, hep-ex/0207043.
- [43] M.Ambrosio et al., Phys. Rev. D67 (2003) 042002, astro-ph/0211119.
- [44] M.Ambrosio et al., Astropart. Phys. 20 (2003) 145, astro-ph/0302586.
- [45] M.Ambrosio et al., Eur. Phys. J. C37 (2004) 265.
- [46] M.Ambrosio et al., Phys. Lett. B566 (2003) 35, hep-ex/0304037.
- [47] EASTOP-MACRO Coll., M.Aglietta et al., Astropart. Phys. 20 (2004) 641.
- [48] EASTOP-MACRO Coll., M.Aglietta et al., Astropart. Phys. 21 (2004) 223.
- [49] M.Ambrosio et al., hep-ex/0402006(2004).
- [50] M.Ambrosio et al., Eur. Phys. J. C36 (2004) 323.
- [51] IMB Coll., R. Becker-Szendy et al., Phys. Rev. D46(1992)372.
- [52] Kamiokande Coll., Y. Fukuda et al., Phys. Lett. B335(1994)237.
- [53] NUSEX Coll., M.Aglietta et al., 23rd ICRC Proc. 2014(1993)446.
- [54] Frejus Coll., K.Daum et al., Z. Phys. C66(1995)417.
- [55] Baksan Coll., S.Mikheyev et al., Phys. Lett. B391 (1997)491; Phys. Lett. B449(1999)137.
- [56] Soudan 2 Coll., W.W.M. Allison et al., Phys. Lett.B391 (1997) 491.
- [57] Soudan 2 Coll., W.W.M. Allison et al., Phys. Lett. B449 (1999) 137; M. Sanchez et al., Phys. Rev. D68(2003)113004.
- [58] SuperKamiokande Coll., Y.Fukuda et al., Phys. Rev. Lett. 81(1998)1562; Phys. Lett. B433(1998)9; Phys. Rev. Lett. 85(2000)3999. Y. Ashie et al., Phys. Rev. Lett. 93(2004)101801.
- [59] MACRO Coll., P. Bernardini, hep-ex/9809003; F. Ronga, hep-ex/9810008.
- [60] K2K Coll., D. Kielorezka et al., Acta Phys. Polon. B35(2004)1453.
MINOS Coll., N. Tagg et al., hep-ex/0605058.
OPERA Coll., R. Acquafredda et al., J. Phys. 8(2006)303. hep-ex/0703247.
- [61] V. Agrawal et al., Phys. Rev. D53(1996)1314.
- [62] M.Honda et al., Phys. Rev. D52(1995)4985.
- [63] M.Honda et al., Phys. Rev. D64(2001)053011; Phys. Rev. D70(2004)043008.
- [64] G. Battistoni et al., Astrop. Phys. 19(2003)269.
- [65] T.K.Gaisser et al., Nucl. Phys. B Proc. Suppl. 118(2003)109.
- [66] L3C Coll., P. Le Coultre et al., BESS Coll., T. Sanuki et al., Proc. of NOW2004, Otranto, 2004.
- [67] G.Giacomelli et al., hep-ex/0201032; hep-ex/0504002; Phys. Atomic Nuclei 67(2004)1139.
- [68] G. Battistoni et al., Phys. Lett. B615(2005)14; hep-ex/0503015; hep-ex/0508041.
- [69] M.C.Gonzalez et al., Phys. Rev. D70(2004)033010.
- [70] S. Cecchini et al., hep-ex/0606037; Astrop. Phys. 21(2001)35.
- [71] N. Fornengo, "New Trends in Neutrino Physics", Ringberg Castle, 1998, World Scient.
- [72] P.A.M. Dirac, Proc. Roy. Soc. 133(1931)60.
- [73] G. 't Hooft, Nucl. Phys. B29(1974)276.
- [74] G. Giacomelli et al., hep-ex/0005041; hep-ex/0506014; hep-ex/0702050.
G. Giacomelli, Rivista Nuovo Cimento 7 N12(1984)1.
- [75] P. B. Price, Phys. Rev. D38(1988) 3813. D. Ghosh et al., Europhys. Lett. 12(1990)25.
- [76] K. A. Milton, Rept. Progr. Phys. 69(2006)1637.
- [77] J. Derkaoui et al., Astropart. Phys. 9(1998)173; Astropart. Phys. 10(1999)339.
- [78] E. Witten, Phys. Rev. D30(1984)272. A. de Rujula and S. Glashow, Nature 31(1984)271.
- [79] S. Coleman, Nucl. Phys. B262(1985)293. A. Kusenko et al., Phys. Lett. B418(1998)46.
- [80] M. Yu. Klopov et al., astro-ph/0603187.
- [81] D. Bakari et al., hep-ex/0004019.
- [82] M. Sioli, hep-ex/0209029; hep-ex/0201017.
- [83] Y. Becherini et al., Astropart. Phys. 23(2005)341, astro-ph/0502251.
- [84] J. Knapp and D. Heck, Extensive Air Shower Simulation with CORSIKA 5.61 (1998).
- [85] S. Cecchini et al., Radiat. Meas. 34(2001)55, hep-ex/0104022.
- [86] S. Nakamura et al., Phys. Lett. B263(1991)529.
- [87] S. Orito et al., Phys. Rev. Lett. 66(1991)1951.
- [88] P. Lipa et al., Phys. Lett. B285(1992)300.
- [89] P. Antonioli et al., Astrop. Phys. 7(1997)357.
- [90] EASTOP Collaboration, M. Aglietta et al., Nucl. Phys. B Proc. Suppl. 54(1997)263.